Nramp1 promotes efficient macrophage recycling of iron following erythrophagocytosis in vivo

Shan Soe-Lin[a,b], Sameer S. Apte[b], Billy Andriopoulos, Jr.[c], Marc C. Andrews[d], Matthias Schranzhofer[b,e], Tanya Kahawita[b,e], Daniel Garcia-Santos[b], and Prem Ponka[a,b,e,1]

[a]Division of Experimental Medicine and [e]Department of Physiology, McGill University, Montreal, QC, Canada H3A 2T5; [b]Lady Davis Institute for Medical Research, Jewish General Hospital, Montreal, QC, Canada H3T 1E2; [c]Program in Membrane Biology, Division of Nephrology, Center for Systems Biology, Massachusetts General Hospital, Harvard Medical School, Boston, MA 02114; and [d]Department of Molecular Genetics and Development, Institut de Recherches Cliniques de Montreal, Montreal, QC, Canada H2W 1R7

Edited by Solomon H. Snyder, Johns Hopkins University School of Medicine, Baltimore, MD, and approved February 18, 2009 (received for review January 23, 2009)

Natural resistance-associated macrophage protein 1 (Nramp1) is a divalent metal transporter expressed exclusively in phagocytic cells. We hypothesized that macrophage Nramp1 may participate in the recycling of iron acquired from phagocytosed senescent erythrocytes. To evaluate the role of Nramp1 in vivo, the iron parameters of WT and KO mice were analyzed after acute and chronic induction of hemolytic anemia. We found that untreated KO mice exhibited greater serum transferrin saturation and splenic iron content with higher duodenal ferroportin (Fpn) and divalent metal transporter 1 (DMT1) expression. Furthermore, hepatocyte iron content and hepcidin mRNA levels were dramatically lower in KO mice, indicating that hepcidin levels can be regulated by low-hepatocyte iron stores despite increased transferrin saturation. After acute treatment with the hemolytic agent phenylhydrazine (Phz), KO mice experienced a significant decrease in transferrin saturation and hematocrit, whereas WT mice were relatively unaffected. After a month-long Phz regimen, KO mice retained markedly increased quantities of iron within the liver and spleen and exhibited more pronounced splenomegaly and reticulocytosis than WT mice. After injection of ^{59}Fe-labeled heat-damaged reticulocytes, KO animals accumulated erythrophagocytosed ^{59}Fe within their liver and spleen, whereas WT animals efficiently recycled phagocytosed ^{59}Fe to the marrow and erythrocytes. These data imply that without Nramp1, iron accumulates within the liver and spleen during erythrophagocytosis and hemolytic anemia, supporting our hypothesis that Nramp1 promotes efficient hemoglobin iron recycling in macrophages. Our observations suggest that mutations in *Nramp1* could result in a novel form of human hereditary iron overload.

hemolytic anemia | iron overload | iron homeostasis | hepcidin | ferroportin

Reticuloendothelial macrophages are critical in the maintenance of iron homeostasis (1). Nearly 80% of bodily iron is found in hemoglobin within erythrocytes, which when senescent are phagocytosed at the rate of ≈2 million/sec by macrophages of the reticuloendothelial system (2). Each day, these macrophages quickly and efficiently recycle 25 mg of erythrocyte-derived iron and ensure its export to the plasma. Subsequently, iron binds to transferrin and is shuttled to the bone marrow for use in erythropoiesis (3–5). Any disturbances in this normally efficient and tightly regulated process can result in anemia of chronic disease (6–9), iron overload (10), or other pathologies (11, 12).

Hepcidin is an antimicrobial peptide that regulates organismal iron homeostasis. By binding to and inducing the degradation of ferroportin (13), the only known cellular iron exporter (14–16), hepcidin inhibits dietary iron absorption and prevents the release of iron from reticuloendothelial macrophages (17). A loss of hepcidin gene expression in both mice and humans results in iron overload (18, 19), whereas an excess of hepcidin gene expression in mice results in severe iron-deficiency anemia (20, 21). Hepcidin synthesis is stimulated by iron and inflammatory stimuli (22–25), but decreased by factors including anemia and hypoxia (23). Increased hepcidin expression caused by inflammation is believed to be the primary pathogenic mechanism in anemia of chronic disease (9, 26–28). Lastly, GDF15, a humoral factor produced by red-blood-cell precursors, has been shown to decrease the production of hepcidin, but only under the pathological setting of β-thalassemia (29).

The pathways by which a decrease in hepcidin occurs are yet to be fully elucidated; however, there is substantial evidence to suggest the existence of a "stores regulator" that decreases hepcidin production in response to low iron and a separate "erythroid regulator" (30) that decreases hepcidin production via an unknown, yet distinct mechanism during conditions which require a high rate of erythropoiesis (31, 32). Thus, hepcidin has the ability to decrease intestinal iron absorption and macrophage iron release when the demand for iron has been met, while augmenting iron availability for erythropoiesis when the need for iron is increased.

Nramp1 is a divalent metal transporter expressed within the late endosomal and phagolysosomal membranes of iron-recycling macrophages and other professional phagocytes (33, 34). G169D mutations in *Nramp1* result in increased susceptibility to intracellular pathogens (35, 36). Nramp1 is thought to confer protection against microbes by depleting the phagolysosome of iron needed by the pathogen for growth (37) and by decreasing intracellular iron availability, thereby stimulating the production of nitric oxide (38), a potent antimicrobial effector. In addition to promoting host resistance, we (39) and others (40) have observed that Nramp1 increases the recycling efficiency of erythrocyte-derived iron in macrophages.

Unlike mutations in divalent metal transporter 1 (DMT1, Nramp2), which cause severe microcytic anemia (41–45), mutations in Nramp1 have not been found to cause severe anemia in mice (Philippe Gros, personal communication). Nevertheless, we hypothesize that the effects of Nramp1 deficiency may become more apparent during conditions of accelerated erythrophagocytosis. In this study, iron parameters were measured in WT 129Sv (Nramp1$^{+/+}$) and congenic 129Sv KO mice (Nramp1$^{-/-}$) after hemolytic anemia induced by acute or chronic phenylhydrazine treatment. A deficiency in Nramp1 resulted in impaired recovery from anemia in all KO groups. Moreover, the untreated KO animals were found to have dramatically decreased hepcidin mRNA levels and proceeded to develop progressive reticuloendothelial iron overload with age. This finding is consistent with the

Author contributions: S.S.-L. and P.P. designed research; S.S.-L., S.S.A., B.A., M.C.A., M.S., T.K., and D.G.-S. performed research; S.S.-L., B.A., M.C.A., and P.P. analyzed data; and S.S.-L. wrote the paper.

The authors declare no conflict of interest.

This article is a PNAS Direct Submission.

[1]To whom correspondence should be addressed at: Lady Davis Institute for Medical Research, 3755 Côte Ste-Catherine Road, Montreal, QC, Canada H3T 1E2. E-mail: prem.ponka@mcgill.ca.

This article contains supporting information online at www.pnas.org/cgi/content/full/0900808106/DCSupplemental.

Table 1. Iron parameters of mice not treated with phenylhydrazine

	Nramp1$^{+/+}$, 5 wks	Nramp1$^{-/-}$, 5 wks	Nramp1$^{+/+}$, 9 months	Nramp1$^{-/-}$, 9 months
Hepcidin mRNA, arbitrary units normalized to control	1 ± 0.09	0.063*** ± 0.002	0.94 ± 0.04	0.057*** ± 0.003
Transferrin saturation, %	64 ± 7.6	84* ± 5.4	59 ± 3.6	80* ± 1.0
Spleen index	0.0029 ± 1.4 × 10^{-5}	0.0029 ± 1.3 × 10^{-5}	0.0026 ± 0.0003	0.0046* ± 0.001
Splenic iron content, μg/g wet weight	953.8 ± 65.81	1102.3* ± 58.93	1035.8 ± 38.4	1265.8* ± 25.2
Liver iron content, μg/g wet weight	138.6 ± 1.9	147.8 ± 5.3	154.2 ± 3.9	192.4** ± 4.4
Hematocrit, %	45.3 ± 1.2	44.2 ± 3.9	44.1 ± 1.4	43 ± 1.1
Plasma erythropoietin, mU/ml	1.48 ± 0.15	2.64* ± 0.27	NA	NA
Hepatocyte nonheme iron content, μg per 10^6 cells	0.026 ± 0.0014	0.017* ± 0.0035	NA	NA

*, $P \leq 0.05$; **, $P \leq 0.01$; ***, $P \leq 0.0001$; $n = 6–8$. NA, not available.

hypothesis that Nramp1 plays an active role in macrophage recycling of iron derived from the phagocytosis of senescent erythrocytes.

Results

Iron Homeostasis and Hepcidin Expression in WT and KO Animals. To investigate the role of Nramp1, we evaluated several parameters of iron homeostasis in untreated 5-week-old WT (Nramp1$^{+/+}$) and congenic KO (Nramp1$^{-/-}$) 129Sv mice (Table 1). We found that the nonheme iron content of freshly isolated hepatocytes and hepcidin mRNA levels were strikingly lower in untreated KO mice than WT controls. Although the spleen indices (defined as the spleen/body weight ratio) and hematocrits were nearly identical in both groups, the splenic iron content was significantly higher in the KO animals. The nonheme iron content of the liver [comprised of both hepatocytes and macrophages (4, 46)] was also elevated in KO animals, although not to a statistically significant degree. The 129Sv/J strain is a "high-iron" strain; our measurements of nonheme iron in the spleen and liver are consistent with other published reports by using this background (18, 47). In addition to markedly lower hepcidin mRNA levels, the KO animals exhibited elevated transferrin saturation as compared with WT controls (84% vs. 64%, respectively). Although the splenic index and hematocrits were virtually identical in untreated 5-week- and 36-week-old WT animals, the nonheme iron contents of both the spleen and liver were significantly increased in the 36-week-old KO animals as compared with 36-week-old controls.

These results are consistent with a defect in Nramp1 leading to inefficient recycling of erythrophagocytosed iron and retention of iron within reticuloendothelial cells. We hypothesize that hepatocytes' iron stores are released to compensate for the lack of iron released from macrophages, resulting in a lower production of hepcidin mRNA. Sustained under-production of hepcidin, combined with an impaired ability of macrophages to release iron, would lead to the progressive iron retention we observed in older Nramp1$^{-/-}$ mice.

Iron Homeostasis After Acute Hemolytic Anemia. Although Nramp1 deficiency results in only mild pathology under normal conditions (Table 1), we hypothesize that when erythropoietic demand for recycled iron is increased, the effects of Nramp1 deficiency may become more pronounced. Accordingly, hemolytic anemia was induced in WT and KO animals with phenylhydrazine, a well-characterized model of erythropoietic stress (48, 49). After the acute induction of hemolytic anemia, KO animals exhibited impaired erythropoietic recovery (Table 2). Both WT and KO mice treated with phenylhydrazine developed anemia with increased reticulocyte counts (22.5% in WT and 31.3% in KO; $P < 0.05$) and decreased mean cell volume; however, the hematocrit and transferrin saturation were significantly decreased in the KO cohort. Furthermore, nonheme iron in the liver and spleen was also elevated to a greater degree in the KO animals. This effect was likely because of greater retention of iron within hepatic and splenic macrophages.

Previous studies indicate a minimum 4-day delay between phenylhydrazine-induced hemolysis and a corresponding increase in iron absorption (50). During this lag period, iron for erythropoiesis must come exclusively from iron stores. To separate the effects of Nramp1 deficiency from a possible compensatory up-regulation in dietary iron absorption, WT and KO animals were injected with phenylhydrazine on 2 consecutive days (as in the acute experiment) and maintained on an iron-deficient diet immediately after the first injection. KO mice experienced a significant decrease in transferrin saturation, whereas WT animals were relatively unaffected (Table 2). These observations indicate that KO animals were at a considerable disadvantage when forced to depend exclusively on stored iron for their erythropoietic needs.

Iron Homeostasis After Chronic Hemolytic Anemia. To further examine the long-term effects of Nramp1 deficit on iron homeostasis, the iron parameters of WT and KO mice after chronic, low-dose phenylhydrazine administration were examined (Table 3). As in the acute experiments, chronic administration of phenylhydrazine resulted in mild anemia in both cohorts, with a statistically significant decrease in hematocrit in KO mice (please compare Table 3 with untreated values from Table 1). Transferrin saturation in KO mice was also significantly lower after chronic phenylhydrazine treatment. This depletion of transferrin iron in both KO and WT mice likely results from the increased erythropoietic demand for iron. Hepatic hepcidin mRNA levels were dramatically decreased in phenylhydrazine-treated WT and KO mice (Table 3) in comparison with untreated mice (Table 1). Additionally, significantly elevated

Table 2. Iron parameters following acute phenylhydrazine-treated mice

	Nramp1$^{+/+}$	Nramp1$^{-/-}$
Transferrin saturation, normal iron diet, %	59 ± 5.2	38* ± 3.6
Transferrin saturation, low iron diet, %	56.2 ± 4.6	31.4* ± 2.3
Spleen index	0.015 ± 0.0027	0.021* ± 0.0035
Splenic iron content, μg/g wet weight	1236.4 ± 46.2	1487.4* ± 65.1
Liver iron content, μg/g wet weight	290.3 ± 14.2	310.4 ± 32.5
Hematocrit, %	27.4 ± 4.9	22.2* ± 3.1
Plasma erythropoietin, mU/ml	43.3 ± 6.7	207.9** ± 41.4

Acute hemolytic anemia was induced in 5-week-old Nramp1$^{+/+}$ and Nramp1$^{-/-}$ mice with 2 consecutive daily 50 mg/kg injections of phenylhydrazine (Phz). The mice were killed 48 h after the last injection, and their iron parameters were evaluated. Unless otherwise specified, animals were maintained on an iron-replete diet (*, $P \leq 0.05$; **, $P \leq 0.01$; $n = 6–8$).

PHYSIOLOGY

Table 3. Iron parameters of chronic phenylhydrazine-treated mice

	Nramp1$^{+/+}$	Nramp1$^{-/-}$
Hepcidin mRNA, arbitrary units normalized to control	0.04 ± 0.001	0.008* ± 0.0002
Transferrin saturation, %	37 ± 5.3	28* ± 5.8
Spleen index	0.017 ± 0.0021	0.021* ± 0.0009
Splenic iron content, μg/g wet weight	1167.9 ± 42.2	1408.1* ± 31.9
Liver iron content, μg/g wet weight	228.3 ± 18.4	260.4 ± 26.9
Hematocrit, %	35.4 ± 1.7	30.7* ± 2.1
Plasma erythropoietin, mU/ml	103.8 ± 12.5	203.48** ± 9.7

Chronic hemolytic anemia was induced in 5-week-old Nramp1$^{+/+}$ and Nramp1$^{-/-}$ mice with biweekly injections of 25 mg/kg of phenylhydrazine (Phz) for 4 weeks. The mice were killed, and their iron parameters were evaluated (*, $P \leq 0.05$; **, $P \leq 0.01$; $n = 6–8$).

levels of nonheme iron retained within the livers and spleens were observed, as well as a marked degree of splenomegaly in KO mice as compared with their WT counterparts. These results imply a significant impairment of iron recycling in macrophages lacking functional Nramp1.

Retention of Erythrophagocytosed Iron by Splenic Macrophages in KO Mice. To visualize the location of iron deposits, Perls' staining was performed on liver [supporting information (SI) Fig. S1] and spleen (Fig. 1) sections. Although there was a minor increase of blue iron deposits within the liver Kupffer cells of the KO animals, the distinction did not reach significance (Fig. S1); however, striking differences in stainable iron were noted among the splenic samples (Fig. 1). Morphologic analysis showed that the KO mice contained significant iron deposits within their splenic macrophages from as early as 5 weeks of age. Conversely, virtually no iron deposits were detectable in WT animals of the same age (Fig. 1*A*). Iron-positive blue deposits were extensively distributed throughout the splenic macrophages of 36-week-old KO animals, whereas iron levels were minimally increased in WT controls (Fig. 1*B*). Although iron deposits were apparent in splenic macrophages from both types of mice after chronic phenylhydrazine treatment, they were found to a much greater degree in KO animals (Fig. 1*C*). Fig. 1*D* shows the percentage of area staining positive for iron relative to the whole field.

DMT1 and Ferroportin Protein Expression Is Greatly Increased in both Untreated and Chronic Phenylhydrazine-Treated KO Mice. To assess the potential of KO and WT mice to absorb iron from the diet, duodenal DMT1 and ferroportin protein levels were examined. DMT1 and ferroportin protein levels were dramatically increased in untreated and treated KO animal duodenums when compared with their counterpart WT mice (Fig. 2). The increased intestinal DMT1 and ferroportin levels observed in KO mice, both under untreated and chronic phenylhydrazine treatment conditions, indicate that dietary iron absorption is greatly increased in KO mice. This observation strongly suggests an increase in dietary iron absorption in KO mice to compensate for the impaired release of iron from erythrophagocytosing macrophages and accounts for the increased transferrin saturation level observed in the KO animals. Furthermore, we observed that splenic macrophage ferroportin was also greatly elevated in untreated KO animals as compared with WT (Fig. 2*D*). Despite this fact, iron was still retained within spleens of KO mice, indicating that the absence of Nramp1 limits the amount of iron available for export by ferroportin in macrophages.

Nramp1 KO Mice Experience Increased Retention of ^{59}Fe Within Their Liver and Spleen After Injection of Heat-Damaged ^{59}Fe-Labeled Reticulocytes. To directly assess the effect of Nramp1 on the recycling of hemoglobin iron, WT and KO mice were injected i.p. with

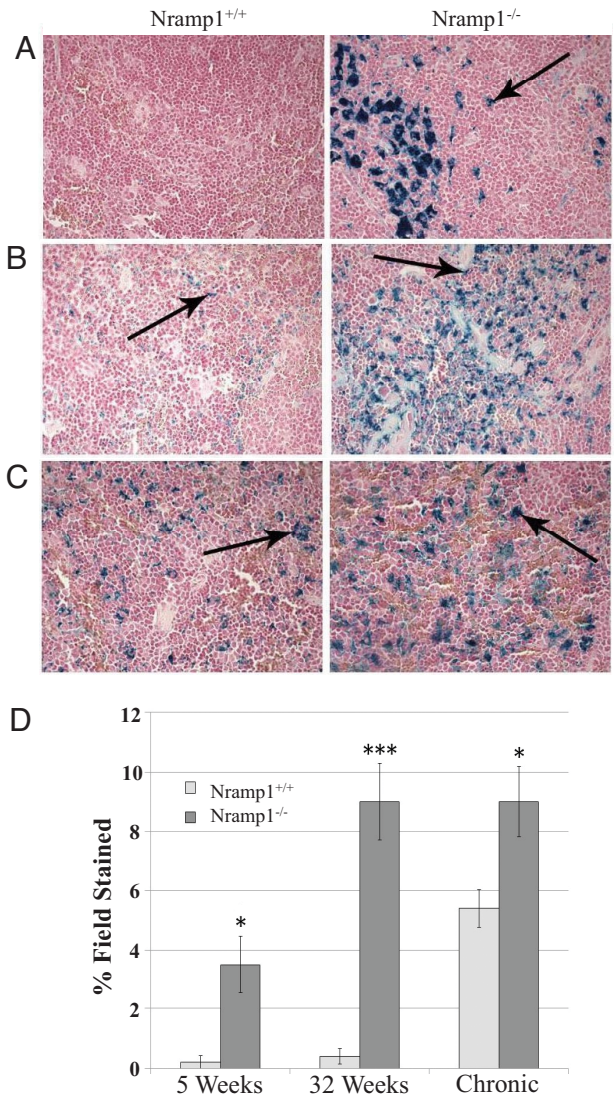

Fig. 1. Impaired recycling of erythrocyte-derived iron by splenic macrophages in KO mice. Perls' Prussian blue staining was performed to visualize the location of iron deposits within the spleen. Hematoxylin and eosin counterstains were used. Arrows point to blue iron-positive deposits and show localization of iron to splenic macrophages (*A*), 36-week-old mice (*B*), and chronically phenylhydrazine-treated mice (*C*). Three representative nonoverlapping fields were scored for blue iron-positive deposits (indicated by arrows). Areas staining positive for iron were converted to pixels, quantified with Northern Eclipse 6.0 software, and expressed as a percentage of the total surface area of the field (*D*). *, $P < 0.05$; ***, $P < 0.001$.

^{59}Fe-labeled heat-damaged reticulocytes, which are detected and preferentially phagocytosed by reticuloendothelial macrophages (3). Initial pilot experiments were consistent with previous reports (51–53), which indicated that undamaged erythrocytes injected i.p. travel intact into the circulation within 24 h (Fig. 3*A*). Furthermore, there was no difference in the ability of KO and WT animals to absorb i.p. injected ^{59}Fe-transferrin and incorporate it into developing blood cells (Fig. S2). The passage of phagocytosed ^{59}Fe from reticuloendothelial macrophages of the liver and spleen to the plasma, and eventually to the bone marrow, was monitored over time. Over all time points (Fig. 3*B*), more ^{59}Fe was consistently found in the red blood cells, plasma, and marrow compartments of WT animals, whereas KO animals retained more ^{59}Fe in their liver and spleen. The amount of phagocytosed ^{59}Fe retained within the liver and spleen decreased in WT animals with time, whereas KO

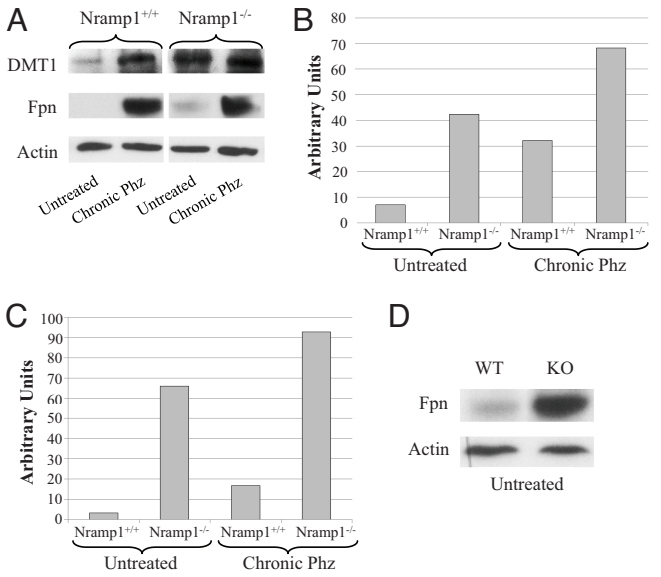

Fig. 2. DMT1 and ferroportin protein expression are greatly increased in both untreated and chronic phenylhydrazine-treated KO mice. Tissue from the proximal 2 cm of the duodenum was collected from untreated and chronic phenylhydrazine-treated mice, and Western blots for DMT1 and ferroportin were performed (*A*). Relative protein levels for DMT1 (*B*) and Fpn (*C*) were determined with densitometry analysis. Splenic macrophages were isolated from untreated mice and probed as above for Fpn (*D*). Results are representative of at least 3 independent experiments.

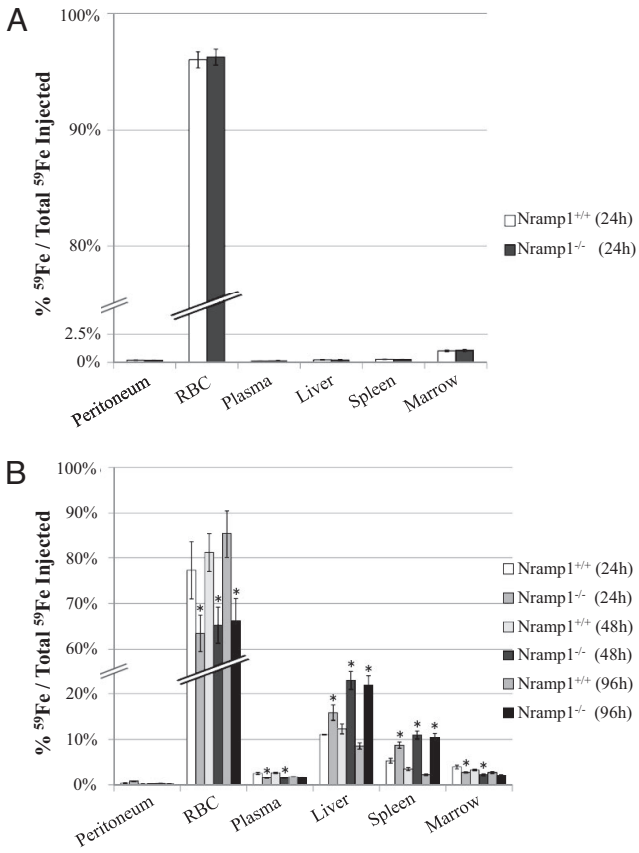

Fig. 3. Bodily distribution of injected ^{59}Fe. In *A*, mice were injected with ^{59}Fe-Tf and blood and organs were collected after 24 h. In *B*, mice were fed an iron-deficient diet and injected with ^{59}Fe-labeled opsonized erythrocytes 12 days later. Mice were killed 24 h, 48 h, and 96 h following the injection. In all cases, the ^{59}Fe contained within each compartment was assessed via gamma counting and expressed as a percentage of the total ^{59}Fe initially injected. At least 3 animals were used per group. *, $P < 0.05$.

animals were less able to release the iron trapped within these organs. These findings provide direct evidence that the loss of Nramp1 results in a diminished release of erythrophagocytosed iron from macrophages, leading to iron retention within hepatic and splenic macrophages and to a decrease in the availability of erythrocyte-derived iron for erythropoiesis.

Discussion

Previously, we showed that Nramp1 equips macrophages for efficient recycling of iron in both cell line and primary macrophage cultures (39). Here, we demonstrate that macrophage Nramp1 also plays a significant role in the recovery of iron from erythrocytes in vivo during conditions of increased erythrophagocytosis.

Macrophages are fundamental components of the innate immune system because of their critical role in the surveillance and removal of harmful pathogens. In a much less heralded, but equally vital role, macrophages are responsible for recycling hemoglobin iron acquired from the phagocytosis of senescent erythrocytes. Importantly, the amount of iron in macrophages available for erythropoiesis is limited by increased hepcidin levels (17, 26). Prolonged inflammation and subsequent hepcidin expression can also lead to iron retention within macrophages and eventually to anemia of chronic disease (9, 26–28, 54).

To build on our previous in vitro studies of Nramp1 (39), we sought to characterize Nramp1$^{-/-}$ (KO) and Nramp1$^{+/+}$ (WT) mice. We found that 5-week-old KO mice had greater iron loading, as measured chemically, in the liver and spleen than WT mice (Table 1). These untreated KO mice developed progressive iron overload as they aged (Table 1), as evidenced by the marked increase of splenic and liver iron content, quantified chemically by the ferrozine assay and its location visualized by the Perls' stain. Although the stainable iron identified by the Perls' stain appears to be much greater than what was measured by ferrozine, it should be kept in mind that the Perls' stain is a qualitative assay (55). Whereas the ferrozine assay measured moderate iron loading of the spleen in KO mice, the Perls' staining showed the retained iron to be localized within splenic macrophages. In contrast to untreated KO mice, WT mice exhibited relatively little progressive iron loading with age. The significant amount of splenic rather than hepatic iron deposits in KO animals suggests that the majority of erythrophagocytosis likely occurs within the spleen in mice. Our previous findings demonstrated that Nramp1-deficient macrophages released a modest 7% less iron than Nramp1-replete macrophages after erythrophagocytosis (39). The observations presented in this report, showing progressive iron loading of the spleen and liver with increasing age in KO mice, suggest that even a minor decrease in iron-recycling efficiency in macrophages can lead to significant cumulative pathology over time.

Untreated 5-week-old KO animals displayed increased transferrin saturation. Despite this, hepatocytes were iron depleted, and, likely as a result of this depletion, hepcidin mRNA levels were markedly decreased (Table 1). This observation indicates that hepcidin levels can be regulated by low hepatocyte iron stores despite increased transferrin saturation, in contrast to the current belief that transferrin saturation is the major regulator of hepcidin synthesis (56). We hypothesize that hepatocytes in KO animals release iron stores to compensate for impaired macrophage iron release and reduce the production of hepcidin mRNA accordingly. The observed increases in DMT1 and ferroportin within the duodenums of the KO animals imply that the seemingly paradoxical increase in transferrin saturation, despite impaired iron release from reticuloendothelial macrophages, occurs because of a compensatory increase in dietary iron absorption (Fig. 4). Furthermore,

PHYSIOLOGY

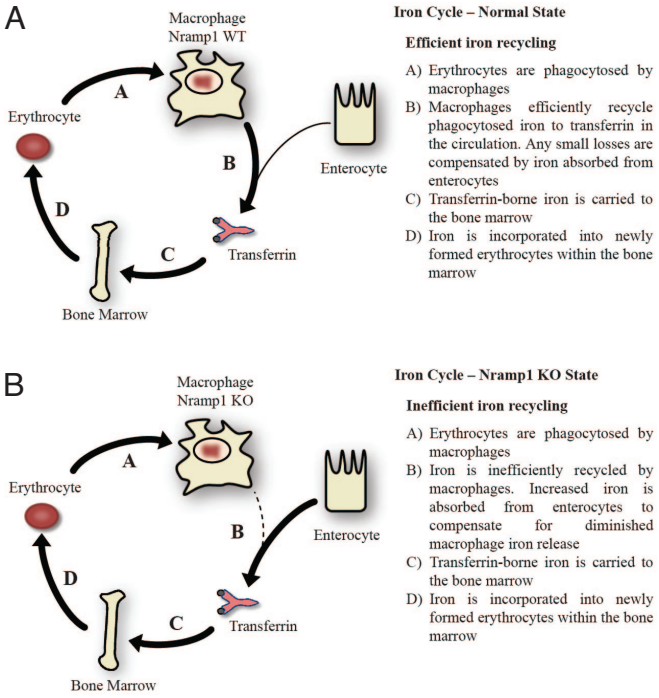

Fig. 4. Scheme of iron-recycling pathway within WT and Nramp1-KO mice. Schemes show normal-state efficient iron recycling (*A*) and Nramp1-KO-state inefficient iron recycling (*B*).

the observed impairment in macrophage iron release in KO animals, despite increased splenic ferroportin expression, indicates that Nramp1 is important in making iron available for export by ferroportin in macrophages (Fig. 2*D*). It needs to be pointed out that Nramp1 functions proximally to ferroportin.

We found KO animals to be at a significant disadvantage after enhanced erythrophagocytosis caused by phenylhydrazine-induced hemolytic anemia. Although the erythroblast population was relatively unchanged (Fig. S3) after acute induction of hemolytic anemia, transferrin saturation and hematocrit were markedly decreased, whereas the splenic index and iron content of both the spleen and liver were dramatically increased (Table 2). Furthermore, KO mice placed on an iron-restricted diet experienced an even more precipitous decrease in transferrin saturation than WT mice after acute hemolytic anemia. These KO mice were forced to rely entirely on stored iron because of dietary insufficiency, but could not meet the increased erythropoietic demand because of Nramp1 deficiency.

As compared with WT animals, radioactive iron was found to accumulate in the spleen and the liver of KO animals after the injection of heat-damaged ^{59}Fe-labeled reticulocytes (Fig. 3*B*). In contrast, erythrophagocytosed ^{59}Fe was efficiently released from the spleen and liver of WT animals and subsequently transported to the bone marrow. These observations are consistent with our hypothesis that the absence of Nramp1 results in a marked retention of iron within macrophages and a decrease in the availability of recycled iron for erythropoiesis.

It is expected that an analogous mutation in human *Nramp1*, if found, would result in a pattern of iron overload similar to patients with decreased iron export from macrophages caused by loss-of-function mutations in ferroportin (10, 46, 57). In fact, patients with the phenotype corresponding to loss-of-function mutations in ferroportin, but without defects in the ferroportin gene, have been identified (Antonello Pietrangelo, personal communication). This finding raises the intriguing possibility that human mutations of Nramp1 may be responsible for the unique type of reticuloendothelial iron overload observed in these patients.

Iron trafficking through the reticuloendothelial system is very dynamic. Hence, a small decrease in iron-recycling efficiency can have profound cumulative effects over time. Whereas the absence of Nramp1 under conditions of normal iron homeostasis results in an apparently well-tolerated slight iron loading of the spleen and liver, phenylhydrazine insult in Nramp1$^{-/-}$ mice results in a significant deficit in iron available for erythropoiesis when compared with Nramp1$^{+/+}$ animals. Although Nramp1 plays a significant role in conferring resistance to intracellular pathogens, it is equally important in the maintenance of iron homeostasis. The findings in this study and others (40) provide further evidence that Nramp1 helps to promote the efficient recycling of erythrocyte-derived iron in macrophages and raises the possibility of the existence of a novel form of human hereditary iron overload.

Methods

A more detailed description of experimental procedures can be found in *SI Results*.

Materials. Anti-DMT1 antibody was a kind gift from Philippe Gros (McGill University, Montreal). Anti-ferroportin antibodies were obtained from Alpha Diagnostics. All other chemicals and reagents were from Sigma unless otherwise specified.

Animals and Tissue Collection. Female WT 129Sv mice expressing Nramp1 (Nramp1$^{+/+}$) were purchased from Charles River Laboratories. Congenic mutant mice, bearing a null Nramp1 mutation (Nramp1$^{-/-}$), were a kind gift from Philippe Gros (35, 36). Two i.p. injections of neutralized phenylhydrazine were administered on 2 consecutive days for the acute experiments (50 mg/kg) or as biweekly (25 mg/kg) injections for the chronic experiments, which lasted for 4 weeks. Control animals were injected with an equivalent volume of sterile saline (0.15 N). At the end of the experimental period, the animals were anesthetized with avertin (1 ml of 2.5% avertin), and whole blood was collected via cardiac puncture with heparin as an anticoagulant. Erythropoietin levels were measured by using a human erythropoietin ELISA kit (R&D Systems), which cross-reacts with mouse erythropoietin. Mouse erythropoietin was used as a standard. Serum iron levels and total iron-binding capacity were determined by using a Sigma total iron-binding capacity (TIBC) kit. Iron-deficient rodent chow TD.80396 was purchased from Harlan Teklad. All animal experiments were approved by the McGill University animal ethics committee.

Determination of Nonheme Iron. Quantification of liver and splenic nonheme iron was carried out by using the ferrozine assay as previously described (58, 59).

Determination of Hepatocyte Iron Content. Primary hepatocytes were elicited from mice by using a Krebs–Henseleit solution/collagenase perfusion protocol as described by Amaxa Biosystems. The isolated hepatocytes were counted in a hemocytometer, and the nonheme iron in the resulting hepatocyte cell pellet was analyzed via the ferrozine assay.

Organ Pathology and Tissue Iron. The spleen index was expressed as a ratio of spleen weight to total body weight. To visualize pathological iron deposits, Perls' Prussian blue staining was performed on liver and spleen sections as previously described (59, 60), viewed with a Zeiss Axiophot image analysis microscope, and quantified with Northern Eclipse 6.0.

RNA Isolation, cDNA Synthesis, and Quantitative Real-Time RT-PCR. Determination of hepcidin mRNA levels, including primers used, was performed as previously described (61).

Western Blot Analysis. Duodenal protein collection and lysis was performed as previously described (16). Spleens were dissociated as previously described (62), and macrophages were enriched by adherence to plastic. Protein was quantified with the Bradford Assay by using Bio-Rad Protein assay reagent. A Western blot was performed by using 75 μg (for ferroportin) and 30 μg (for DMT1 and actin) of protein and its corresponding primary antibodies. An enhanced chemiluminescence Western blotting detection system (GE Lifesciences)

was used for visualization. Densitometry analysis was performed by using ImageQuant 5.0 software.

Preparation of ^{59}Fe-Labeled Heat-Damaged Reticulocytes. ^{59}Fe-labeled reticulocytes were generated as previously described (39) and heat-damaged by incubation at 46 °C for 9 min.

^{59}Fe Recycling Studies. Recipient WT and Nramp1 KO 129/Sv mice were fed an iron-deficient diet for 12 days before receiving a single i.p. injection with 200 μl (80% hematocrit) of labeled, heat-damaged erythrocytes at the start of the experiment. After each time point, the mice were anesthetized with avertin as described above, and their peritoneal cavity washed with 1 ml of PBS; the radioactivity of the resulting wash fluid was measured to verify that all injected red blood cells had been absorbed. Blood (200 μl) was collected into heparinized tubes via cardiac puncture, before perfusion of the whole animal with 30–50 ml of PBS. The peritoneal wash fluid, erythrocytes, plasma, whole liver, whole spleen, and femurs were collected into separate glass tubes, and the radioactivity was measured in a Packard Cobra gamma counter (Global Market Insite, Inc.). The radioactivity within each compartment was calculated as a percentage of the total radioactivity injected. Total blood volume (ml) was estimated as 7% of body weight; the radioactivity contained within the marrow was based on the radioactivity of 2 femurs.

Flow Cytometry. Erythroblasts were isolated from untreated and phenylhydrazine-treated mice as described in Vyoral et al. (62), and the erythropoietic populations were determined as described in Socolovsky et al. (63). Flow cytometry was performed on a Becton Dickinson FACScalibur.

Statistical Analysis. All values are expressed as mean ± SE. Statistical differences between means were determined by using the Student's *t* test (GraphPad software). Data are means ± SE of 3 or 4 mice. All experiments were repeated at least 3 times.

ACKNOWLEDGMENTS. The authors thank Drs. Tomas Ganz, Antonello Pietrangelo, and Mitchell Knutson for their illuminating suggestions and advice; Dr. Philippe Gros (McGill University, Montreal) for his kind gift of mice and antibodies; and Ms. Jing Zhao for her assistance with erythropoietin measurements. This research was funded by grants from the Canadian Institutes of Health Research.

1. Koury MJ, Ponka P (2004) New insights into erythropoiesis: The roles of folate, vitamin B12, and iron. *Annu Rev Nutr* 24:105–131.
2. Sheftel AD, Kim SF, Ponka P (2007) Non-heme induction of heme oxygenase-1 does not alter cellular iron metabolism. *J Biol Chem* 282:10480–10486.
3. Hershko C (1977) Storage iron regulation. *Prog Hematol* 10:105–148.
4. Bothwell TH, Charlton RW, Cook JD, Finch CA (1979) *Iron Metabolism in Man* (Blackwell Scientific, Oxford, UK).
5. Ponka P (1999) Cellular iron metabolism. *Kidney Int Suppl* 69:S2–S11.
6. Kampschmidt RF, Upchurch HF, Johnson HL (1965) Iron transport after injection of endotoxin in rats. *Am J Physiol* 208:68–72.
7. Cartwright GE (1966) The anemia of chronic disorders. *Semin Hematol* 3:351–375.
8. Konijn AM, Hershko C (1977) Ferritin synthesis in inflammation. I. Pathogenesis of impaired iron release. *Br J Haematol* 37:7–16.
9. Weiss G, Goodnough LT (2005) Anemia of chronic disease. *N Engl J Med* 352:1011–1023.
10. Pietrangelo A (2004) The ferroportin disease. *Blood Cells Mol Dis* 32:131–138.
11. Hentze MW, Muckenthaler MU, Andrews NC (2004) Balancing acts: Molecular control of mammalian iron metabolism. *Cell* 117:285–297.
12. Eaton JW, Qian M (2002) Molecular bases of cellular iron toxicity. *Free Radical Biol Med* 32:833–840.
13. Nemeth E, et al. (2004) Hepcidin regulates cellular iron efflux by binding to ferroportin and inducing its internalization. *Science* 306:2090–2093.
14. Abboud S, Haile DJ (2000) A novel mammalian iron-regulated protein involved in intracellular iron metabolism. *J Biol Chem* 275:19906–19912.
15. Donovan A, et al. (2000) Positional cloning of zebrafish ferroportin1 identifies a conserved vertebrate iron exporter. *Nature* 403:776–781.
16. McKie AT, et al. (2000) A novel duodenal iron-regulated transporter, IREG1, implicated in the basolateral transfer of iron to the circulation. *Mol Cell* 5:299–309.
17. Ganz T (2007) Molecular control of iron transport. *J Am Soc Nephrol* 18:394–400.
18. Nicolas G, et al. (2001) Lack of hepcidin gene expression and severe tissue iron overload in upstream stimulatory factor 2 (USF2) knockout mice. *Proc Natl Acad Sci USA* 98:8780–8785.
19. Roetto A, et al. (2003) Mutant antimicrobial peptide hepcidin is associated with severe juvenile hemochromatosis. *Nat Genet* 33:21–22.
20. Nicolas G, et al. (2002) Severe iron deficiency anemia in transgenic mice expressing liver hepcidin. *Proc Natl Acad Sci USA* 99:4596–4601.
21. Du X, et al. (2008) The serine protease TMPRSS6 is required to sense iron deficiency. *Science* 320:1088–1092.
22. Pigeon C, et al. (2001) A new mouse liver-specific gene, encoding a protein homologous to human antimicrobial peptide hepcidin, is overexpressed during iron overload. *J Biol Chem* 276:7811–7819.
23. Nicolas G, et al. (2002) The gene encoding the iron regulatory peptide hepcidin is regulated by anemia, hypoxia, and inflammation. *J Clin Invest* 110:1037–1044.
24. Nemeth E, et al. (2003) Hepcidin, a putative mediator of anemia of inflammation, is a type II acute-phase protein. *Blood* 101:2461–2463.
25. Nemeth E, et al. (2004) IL-6 mediates hypoferremia of inflammation by inducing the synthesis of the iron regulatory hormone hepcidin. *J Clin Invest* 113:1271–1276.
26. Ganz T (2006) Molecular pathogenesis of anemia of chronic disease. *Pediatr Blood Cancer* 46:554–557.
27. Ganz T, Nemeth E (2006) Regulation of iron acquisition and iron distribution in mammals. *Biochim Biophys Acta* 1763:690–699.
28. Theurl I, et al. (2008) Autocrine formation of hepcidin induces iron retention in human monocytes. *Blood* 111:2392–2399.
29. Tanno T, et al. (2007) High levels of GDF15 in thalassemia suppress expression of the iron regulatory protein hepcidin. *Nat Med* 13:1096–1101.
30. Finch C (1994) Regulators of iron balance in humans. *Blood* 84:1697–1702.
31. Pak M, Lopez MA, Gabayan V, Ganz T, Rivera S (2006) Suppression of hepcidin during anemia requires erythropoietic activity. *Blood* 108:3730–3735.
32. Vokurka M, Krijt J, Sulc K, Necas E (2006) Hepcidin mRNA levels in mouse liver respond to inhibition of erythropoiesis. *Physiol Res* 55:667–674.
33. Gruenheid S, Pinner E, Desjardins M, Gros P (1997) Natural resistance to infection with intracellular pathogens: The Nramp1 protein is recruited to the membrane of the phagosome. *J Exp Med* 185:717–730.
34. Forbes JR, Gros P (2003) Iron, manganese, and cobalt transport by Nramp1 (Slc11a1) and Nramp2 (Slc11a2) expressed at the plasma membrane. *Blood* 102:1884–1892.
35. Vidal SM, Malo D, Vogan K, Skamene E, Gros P (1993) Natural resistance to infection with intracellular parasites: Isolation of a candidate for Bcg. *Cell* 73:469–485.
36. Vidal S, et al. (1995) The Ity/Lsh/Bcg locus: Natural resistance to infection with intracellular parasites is abrogated by disruption of the Nramp1 gene. *J Exp Med* 182:655–666.
37. Forbes JR, Gros P (2001) Divalent-metal transport by NRAMP proteins at the interface of host–pathogen interactions. *Trends Microbiol* 9:397–403.
38. Fritsche G, et al. (2007) Modulation of macrophage iron transport by Nramp1 (Slc11a1). *Immunobiology* 212:751–757.
39. Soe-Lin S, Sheftel AD, Wasyluk B, Ponka P (2008) Nramp1 equips macrophages for efficient iron recycling. *Exp Hematol* 36:929–937.
40. Biggs TE, et al. (2001) Nramp1 modulates iron homoeostasis in vivo and in vitro: Evidence for a role in cellular iron release involving de-acidification of intracellular vesicles. *Eur J Immunol* 31:2060–2070.
41. Fleming MD, et al. (1997) Microcytic anaemia mice have a mutation in Nramp2, a candidate iron transporter gene. *Nat Genet* 16:383–386.
42. Canonne-Hergaux F, Zhang AS, Ponka P, Gros P (2001) Characterization of the iron transporter DMT1 (NRAMP2/DCT1) in red blood cells of normal and anemic mk/mk mice. *Blood* 98:3823–3830.
43. Donovan A, et al. (2002) The zebrafish mutant gene chardonnay (cdy) encodes divalent metal transporter 1 (DMT1). *Blood* 100:4655–4659.
44. Mims MP, et al. (2005) Identification of a human mutation of DMT1 in a patient with microcytic anemia and iron overload. *Blood* 105:1337–1342.
45. Iolascon A, et al. (2008) Natural history of recessive inheritance of DMT1 mutations. *J Pediatr* 152:136–139.
46. Donovan A, et al. (2005) The iron exporter ferroportin/Slc40a1 is essential for iron homeostasis. *Cell Metab* 1:191–200.
47. Ten Elshof AE, et al. (1999) Gamma delta intraepithelial lymphocytes drive tumor necrosis factor-alpha responsiveness to intestinal iron challenge: Relevance to hemochromatosis. *Immunol Rev* 167:223–232.
48. Hara H, Ogawa M (1976) Erthropoietic precursors in mice with phenylhydrazine-induced anemia. *Am J Hematol* 1:453–458.
49. Ploemacher RE, van Soest PL (1977) Morphological investigation on phenylhydrazine-induced erythropoiesis in the adult mouse liver. *Cell Tissue Res* 178:435–461.
50. Frazer DM, et al. (2004) Delayed hepcidin response explains the lag period in iron absorption following a stimulus to increase erythropoiesis. *Gut* 53:1509–1515.
51. Jacobson LO, Marks EK, Gaston EO (1959) Studies on erythropoiesis. XII. The effect of transfusion-induced polycythemia in the mother on the fetus. *Blood* 14:644–653.
52. Necas E, Zivny J, Neuwirt J (1972) Effect of polycythemia on erythropoietin production in the hypoxic rat. *Am J Physiol* 223:809–811.
53. Bleiberg I, Perah G, Feldman M (1973) Effect of testosterone on the formation of erythroid spleen colonies from fetal liver precursor cells. *Blood* 41:285–291.
54. Lasocki S, et al. (2008) Phlebotomies or erythropoietin injections allow mobilization of iron stores in a mouse model mimicking intensive care anemia. *Crit Care Med* 36:2388–2394.
55. Culling CFA, Allison RT, Barr WT (1985) *Cellular Pathology Technique* (Butterworths, London).
56. Lin L, et al. (2007) Iron transferrin regulates hepcidin synthesis in primary hepatocyte culture through hemojuvelin and BMP2/4. *Blood* 110:2182–2189.
57. Girelli D, et al. (2008) Clinical, pathological, and molecular correlates in ferroportin disease: A study of two novel mutations. *J Hepatol* 49:664–671.
58. Pountney DJ, et al. (1999) Iron proteins of duodenal enterocytes isolated from mice with genetically and experimentally altered iron metabolism. *Br J Haematol* 105:1066–1073.
59. Szuber N, et al. (2008) Alternative treatment paradigm for thalassemia using iron chelators. *Exp Hematol* 36:773–785.
60. Ferreira C, et al. (2001) H ferritin knockout mice: A model of hyperferritinemia in the absence of iron overload. *Blood* 98:525–532.
61. Kattamis A, et al. (2006) The effects of erythropoetic activity and iron burden on hepcidin expression in patients with thalassemia major. *Haematologica* 91:809–812.
62. Vyoral D, Petrak J, Hradilek A (1998) Separation of cellular iron containing compounds by electrophoresis. *Biol Trace Elem Res* 61:263–275.
63. Socolovsky M, et al. (2001) Ineffective erythropoiesis in Stat5a$^{(-/-)}$5b$^{(-/-)}$ mice due to decreased survival of early erythroblasts. *Blood* 98:3261–3273.